Spatiotemporal Point–Trace Matching Based on Multi-Dimensional Feature Fuzzy Similarity Model

Liu, Yi; Wu, Ruijie; Guo, Wei; Huang, Liang; Li, Kairui; Zhu, Man; van Gelder, Pieter

DOI
10.3390/jmse12101883

Publication date
2024

Document Version
Final published version

Published in
Journal of Marine Science and Engineering

Journal of *Marine Science and Engineering*

MDPI

Article

Spatiotemporal Point–Trace Matching Based on Multi-Dimensional Feature Fuzzy Similarity Model

Yi Liu [1], Ruijie Wu [2,*], Wei Guo [2], Liang Huang [3,4], Kairui Li [2], Man Zhu [5,6,7] and Pieter van Gelder [4]

1 School of Geodesy and Geomatics, Wuhan University, Wuhan 430079, China; yliu@sgg.whu.edu.cn
2 State Key Laboratory of Information Engineering in Surveying, Mapping, and Remote Sensing, Wuhan University, Wuhan 430079, China; guowei-lmars@whu.edu.cn (W.G.); 2015301610360@whu.edu.cn (K.L.)
3 State Key Laboratory of Maritime Technology and Safety, Wuhan University of Technology, Wuhan 430070, China; leung.huang@whut.edu.cn
4 Faculty of Technology, Policy and Management, Delft University of Technology, 2628 BX Delft, The Netherlands; p.h.a.j.m.vangelder@tudelft.nl
5 National Engineering Research Center for Water Transport Safety, Wuhan University of Technology, Wuhan 430070, China; man.zhu.393@whut.edu.cn
6 Intelligent Transportation Systems Research Center, Wuhan University of Technology, Wuhan 430063, China
7 Sanya Science and Education Innovation Park, Wuhan University of Technology, Sanya 572024, China
* Correspondence: jerrywu@whu.edu.cn

Abstract: Identifying ships is essential for maritime situational awareness. Automatic identification system (AIS) data and remote sensing (RS) images provide information on ship movement and properties from different perspectives. This study develops an efficient spatiotemporal association approach that combines AIS data and RS images for point–track association. Ship detection and feature extraction from the RS images are performed using deep learning. The detected image characteristics and neighboring AIS data are compared using a multi-dimensional feature similarity model that considers similarities in space, time, course, and attributes. An efficient spatial–temporal association analysis of ships in RS images and AIS data is achieved using the interval type-2 fuzzy system (IT2FS) method. Finally, optical images with different resolutions and AIS records near the waters of Yokosuka Port and Kure are collected to test the proposed model. The results show that compared with the multi-factor fuzzy comprehensive decision-making method, the proposed method can achieve the best performance (F1 scores of 0.7302 and 0.9189, respectively, on GF1 and GF2 images) while maintaining a specific efficiency. This work can realize ship positioning and monitoring based on multi-source data and enhance maritime situational awareness.

Keywords: ship matching; AIS; remote sensing image; spatiotemporal association; IT2FS

Citation: Liu, Y.; Wu, R.; Guo, W.; Huang, L.; Li, K.; Zhu, M.; van Gelder, P. Spatiotemporal Point–Trace Matching Based on Multi-Dimensional Feature Fuzzy Similarity Model. *J. Mar. Sci. Eng.* **2024**, *12*, 1883. https://doi.org/10.3390/jmse12101883

Academic Editor: Xinqiang Chen

Received: 9 September 2024
Revised: 16 October 2024
Accepted: 17 October 2024
Published: 20 October 2024

1. Introduction

The recognition and tracking of marine ship targets have garnered significant attention in recent years due to their critical role in enhancing maritime situational awareness. These initiatives contribute to maritime traffic safety, fishery regulation, marine resource management, combating illegal fishing, and supporting maritime rescue operations [1]. Remote sensing (RS) images have emerged as reliable data sources for maritime ship detection, driven by advancements in RS imaging technologies. These images provide several advantages, including global accessibility, extensive coverage, regular updates, and the availability of vast amounts of data [2]. Consequently, over the past decade, the number of articles and methods related to ship detection using RS images has increased substantially. Among these methods, deep learning-based techniques have gained popularity [3], including the You Only Look Once series [4] and oriented region convolutional neural networks [5] (oriented R-CNN). However, it is important to acknowledge the limitations of

RS images, such as the extended re-entry period, susceptibility to cloud cover, and inability to reveal the identities of the detected ships.

The limitations of RS images can be partially mitigated by incorporating automatic identification system (AIS) data. AIS utilizes very high-frequency technology to transmit and receive ship locations [6] and offers valuable support and position information [7]. The high timeliness of AIS data can compensate for the lengthy return cycles of RS images. It broadcasts information such as position, speed, course, ship type, and maritime mobile service identity (MMSI) through AIS messages [8], which provide additional details that aid in ship identification and complement the limitations of RS images. However, it is important to note that AIS data have certain limitations in terms of ship identification. First, AIS transponders can be inadvertently or intentionally turned off. For example, vessels engaged in illegal fishing may deliberately disable their AIS transponders before entering no-fishing zones and reactivate them upon departure. As a result, AIS data during these periods may be lost or distorted. Additionally, maritime AIS signals can be influenced by weather conditions, ocean waves, and various electromagnetic factors, leading to data loss, noise, and sparsity in the collected AIS data.

By combining the real-time information provided by AIS data with the extensive coverage and data richness of RS images, a more comprehensive and accurate understanding of maritime activities can be achieved, including tracking, identification, and situational awareness [9,10]. However, traditional methods of ship matching based on RS imagery and AIS trajectories are often performed by setting certain thresholds for time and spatial distances between ships and trajectories to determine if the track points match. This leads to a temporal gap between sensor collection and shipping density, significantly affecting the matching of AIS and remote sensing data [11]. Using fuzzy mathematics-based methods [12] can reduce the uncertainty in point–trace matching by considering the similarity of features across multiple dimensions. However, current research primarily focuses on measuring the similarities of trajectory time and space, which limits the comprehensive characterization of ship trajectory characteristics [13]. Achieving a more comprehensive description of ship trajectories remains challenging in existing research. In addition, current research mainly focuses on using Synthetic Aperture Radar (SAR) images for ship matching, while there is limited research on ship matching using optical remote sensing imagery. SAR images can easily distinguish ships and wakes, whereas ship identification in optical imagery is more influenced by resolution and ship speed [14].

Building on previous research and addressing identified shortcomings, this study proposes a ship-matching model that integrates RS images and AIS data while considering multi-dimensional features. By enriching the extracted features for point–trace matching, the model offers a comprehensive representation of ship trajectories, enabling effective correlation between optical remote sensing imagery and AIS data. The model incorporates four dimensions: space, time, course, and attributes, which describe the relationships between trajectory points and facilitate the association between ship targets in RS images and ship tracks in AIS data. The proposed method incorporates oriented R-CNN techniques to detect ships in RS images automatically [5]. To achieve point–track association, this study employed the interval type-2 fuzzy system (IT2FS) [15]. It enables the mapping of multi-dimensional features to fuzzy sets through variable fuzzification and fuzzy association rules. Finally, the spatiotemporal association between AIS data and RS images was achieved using the Hungarian algorithm, which establishes optimal associations between corresponding points and tracks, thereby facilitating the integration of information from both data sources. Experiments were performed at Yokosuka Port and Kure, Japan, using Gaofen-1 (GF1) and Gaofen-2 (GF2) images. The results show that compared with the multi-factor fuzzy comprehensive decision-making method, the proposed method can achieve the best performance (F1 scores of 0.7302 and 0.9189, respectively, in GF1 and GF2 images), while maintaining a specific efficiency.

The remainder of this paper is organized as follows. Section 2 introduces related research work and Section 3 elaborates on the existing techniques for fusing AIS data and

RS images. Section 4 introduces the proposed methods for extracting multi-dimensional point–track similarity. Section 5 presents an experimental verification and analysis of the proposed approach. Section 6 concludes this paper.

2. Related Works

The inadequacies caused by a single monitoring system can be compensated for by the combining of AIS data and RS images. There are two categories of multi-source data spatiotemporal association methods: statistics-based methods and fuzzy mathematics-based methods.

Most statistical methods use spatial and temporal distance as metrics, with the minimum distance serving as the criterion for evaluating relevance. The mainstream statistical method is Nearest Neighbor [16] and its variants. Nearest Neighbor (NN) compares the spatial distance between the ship location and the track, using the minimum distance as the basis for point–track matching. The distance within the threshold range and the closest distance can be considered to be a successful association. Global Nearest Neighbor [17–19] correlates AIS data and ship position in time and space scales, and calculates the global optimal solution. However, the reliance on NN as a foundational calculation can pose challenges in high-density transportation scenarios. Other statistical methods, such as neural networks [20] and point pattern matching [21], are also available but have seen less development in subsequent research. Neural networks define association as a classification problem, with each pair of targets classified with a neural filter; however, this requires multiple adjustments based on the data. Moreover, the training of a neural network relies on the construction of a matching dataset of ships and trajectories as a basis. In point pattern matching, it takes each observation target as an independent mass point, and uses coherent point set (CPS) analysis to extract the topological relationship and realize multitarget association. However, this method is constrained by its specialized data requirements and limited application scenarios, resulting in relatively poor universality.

Fuzzy mathematic methods are beneficial approaches for addressing uncertainties in data from various sensors. In the study of trajectory association, fuzzy logic can easily realize multi-source data fusion and improve computing efficiency [22], and it is the current mainstream method. The process of fuzzy logic can be divided into four steps. The first step is establishing fuzzy factors, using the fuzzy membership function to express fuzzy factors. Then, it calculates fuzzy factors' weights through logical operations. Combined with fuzzy factors and their weights, the fuzzy sets are obtained to calculate matching results [23]. In these steps, the calculation of the fuzzy factor is important to the result quality, and multi-factor fuzzy comprehensive decision-making [13] is an appropriate method. Multi-factor fuzzy comprehensive decision-making considers the relationship between multi-source data and calculates the fuzzy factor sets of targets, such as distance, bearing, speed, and course. Then, it performs the trajectory association through comprehensive decision-making. In addition, fuzzy clustering is also a feasible method for track association; it converts the trajectory association to solving the membership degree of a multi-source dataset relative to the known center of a cluster. However, incorrect and omissive track correlation occurs in the presence of multiple targets and track intersection, so it is gradually eliminated.

3. Study Areas and Data Sources

In this study, Yokosuka Port, Yokosuka City, and Kure, Hiroshima Prefecture, Japan, were chosen as the experimental areas. GF1 and GF2 images of the port were used for ship detection and association. Five RS images with varying widths were used: 29,200 × 27,620, 35,672 × 34,264, 34,160 × 33,876, 34,160 × 33,856, and 40,456 × 40,104 pixels, including two GF1 images and three GF2 images. Yokosuka Port comprises one GF1 image and two GF2 images, whereas Kure consists of one GF1 image and one GF2 image. The GF1 satellite is the first satellite in China's high-resolution Earth observation system, with a panchromatic spatial resolution of GF1 data of 2 m, and a multispectral spatial resolution

of 8 m. The GF2 satellite is the first civilian optical RS satellite independently developed by China. The panchromatic resolution of the GF2 data is 0.8 m and the multispectral resolution is 3.2 m. More importantly, using Gaofen images, we can obtain the time of image capture, which can be used during matching to filter out data from massive AIS datasets within specific time frames. The thumbnails of the two ports are shown in Figure 1.

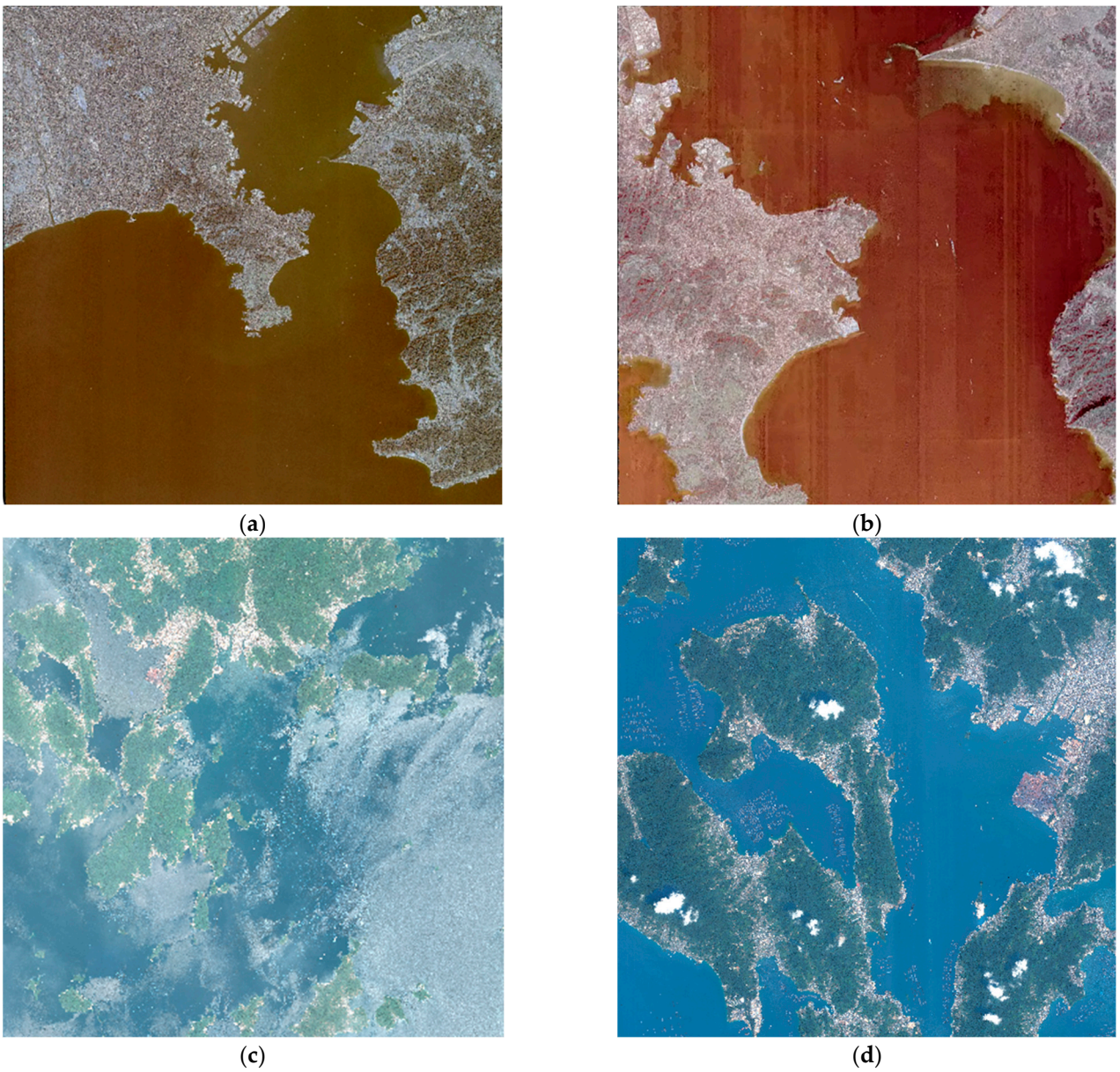

Figure 1. Image thumbnails of the experimental area. (**a**,**b**) are Yokosuka Port, (**c**,**d**) are Kure Port. (**a**,**c**) are GF1 images, (**b**,**d**) are GF2 images.

The AIS data sources were downloaded from Elane and Loong Ships for the period spanning from June 2020 to April 2022, which covered the above GF1 and GF2 images well. Multi-source AIS data can ensure the integrity of the data and avoid the omission of AIS data. To avoid introducing additional uncertainties, we did not use additional linear interpolation on the acquired data to supplement the potential missing data. The AIS data can be divided into dynamic and ship archive data.

The AIS dynamic data mainly contain the trajectory information of ships, including coordinated universal time (UTC), latitude, longitude, course over ground (COG), and speed over ground (SOG). There are 77, 508, 672, and 591 AIS dynamic data points covering

the period from August 2020 to March 2022, with a total of 3,570,966 ships. The ship archive data mainly focused on ship attributes that do not change or are relatively stable, including ship size, type, country, MMSI number, and international maritime organization number. The database contains 445,993 ship file records. The AIS dynamic and ship file information can be linked together according to the MMSI number as it will not change if the ship does not change its country.

4. Research Methods

AISs provide valuable information about the movement trends and identities of ships, while the precise localization capabilities of RS imagery aid in identifying AIS trajectories over large areas. The mutual association between AIS and RS images enhances the understanding of ship activities, offering a more comprehensive view of maritime scenarios. As illustrated in Figure 2, the approach to multi-dimensional point–track association involves using the oriented R-CNN model to detect ship bounding boxes in RS images, with the longitude and latitude of each ship determined through coordinate conversion. Although ship types are not detected, the associated AIS data, which include ship trajectories and attributes, are gathered within the spatial extent of the RS images. Multi-dimensional features—such as space, time [12], course [24], and attributes—are then calculated for ship target points in the RS images and corresponding trajectories in the AIS data. A feature similarity model computes the relationship between the RS images and AIS data. Subsequently, feature fuzzification and fuzzy rules are established to evaluate the similarities between multi-dimensional features and perform point–track matching. Finally, the associated point–tracks with high confidence are the output.

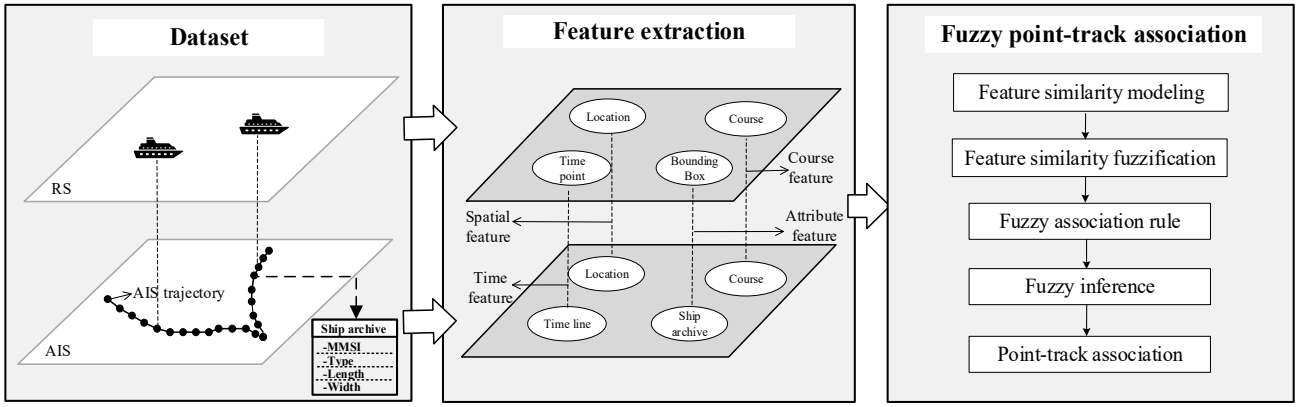

Figure 2. Workflow for point–track association based on multi-dimensional feature similarity.

4.1. Multi-Dimensional Feature Similarity Modeling

Existing studies on the association between RS images and AIS data primarily consider spatiotemporal features and retained certain restrictions on matching accuracy and costly computations [19]. This study considers point–track correlations based on the multi-dimensional features of space, time, course, and attributes.

4.1.1. Spatial Feature Similarity

Spatial feature similarity measures the spatial distance between target points and ship tracks. Each target point is projected onto its corresponding track, generating a reference point on that track. The spatial distance between the target point and its reference point is then used to evaluate the similarity between the spatial features of the target point and the ship track. As the spatial distance decreases, the spatial feature similarity increases, allowing the ship track with the highest spatial feature similarity to be assigned to the target point.

In previous studies, the reference point was the point closest to the target point on the ship track, which could have led to point–track mismatching. In Figure 3a, the red

dots indicate the target points and the green and blue polylines represent the two ship tracks. If the spatial distance is determined using the closest point, the target point is closer to the blue track, as shown in Figure 3b. However, the red point is consistent from a movement standpoint with the intended future routes of the green track. This study offers an alternative method for determining how well the point–track spatial features match. As shown in Figure 3c, the spatial distance between the target point and reference point in the track can offer a precise assessment of how similar the point is to the track.

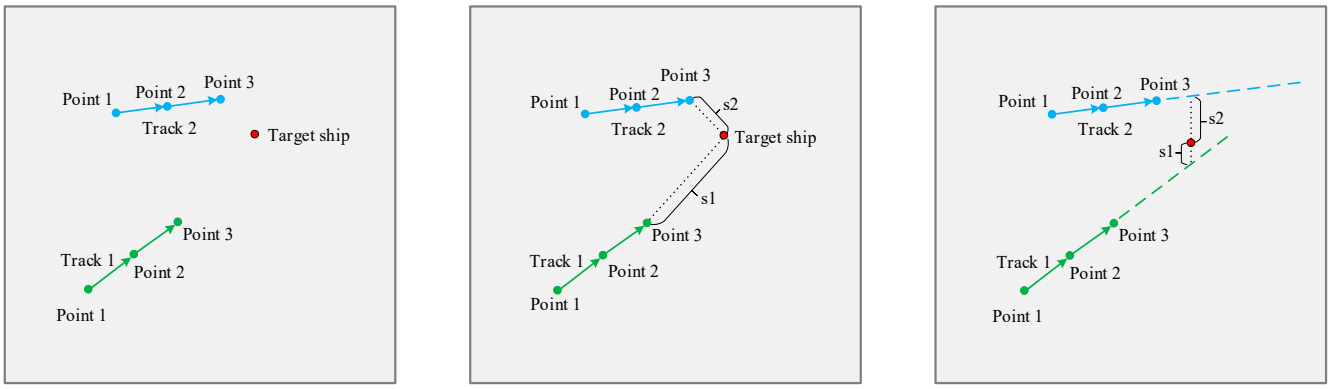

(**a**) (**b**) (**c**)

Figure 3. Drawbacks of directly calculating the spatial distance. The red dots indicate the target points and the green and blue polylines represent the two ship tracks. (**a**) is the initial state, (**b**,**c**) are two different ways of calculating the spatial distance.

To address the inconsistent sampling frequency between RS images and AIS data, this study employs trajectory fitting to establish a reference point in the track for a target point. In normal ship operations, ships often follow a straight-line or arc trajectory. The trajectory fitting process involves creating a univariate polynomial function using a series of trajectory points over a short period, as calculated by the following equations:

$$f(x) = d + \frac{a-d}{1+\left(\frac{x}{c}\right)^b} \tag{1}$$

$$g(x) = ae^{-\frac{(x-b)^2}{2c^2}} \tag{2}$$

where a, b, c, and d are constants. The latitude of the track point is used as the dependent variable y and the longitude of the track point is entered as the independent variable x. When the ship track consists of a small number of points, Equation (1) is considered to be the best-fitting function. In the absence of this equation, the Gaussian fitting function in Equation (2) is used. By adding the current track points to the fitting function, the least-squares method is used to obtain the best values for these four parameters. After parameter estimation, the longitude of the reference point, which is the same as the target point, is entered into the fitting function to obtain the estimated latitude. Therefore, the spatial distance between the reference and target points can be calculated using Equation (3):

$$S = 2 \times arcsin\sqrt{Sin^2\frac{(y_{rp}-y_{tp})}{2} + \left(cos(y_{rp}) \times cos(y_{tp}) \times Sin^2\frac{x_{rp}-x_{tp}}{2}\right)} \times R \tag{3}$$

where S is the spatial distance, R is the Earth's radius, x_{rp} and y_{rp} are the longitude and latitude of the reference point, and x_{tp} and y_{tp} are the longitude and latitude of the target point, respectively.

4.1.2. Time Feature Similarity

Time feature similarity is a measurement of the distance between the image acquisition and trajectory sampling times. It assesses the degree of synchronization in time between the target point and the ship track. Similarly, without temporal features, high spatial feature similarity also leads to mismatched results. As shown in Figure 4, the target point (red dot) and ship track (blue polyline) match with a high spatial feature similarity. However, the timestamp of the target point is between the sampling time of Points 4 and 5, and its position is between Points 3 and 4. This means that the moving ship suddenly turned sharply in the opposite direction and then corrected back to the original direction, which is different from normal ship movement. Therefore, the target point may not belong to the track of the red ship.

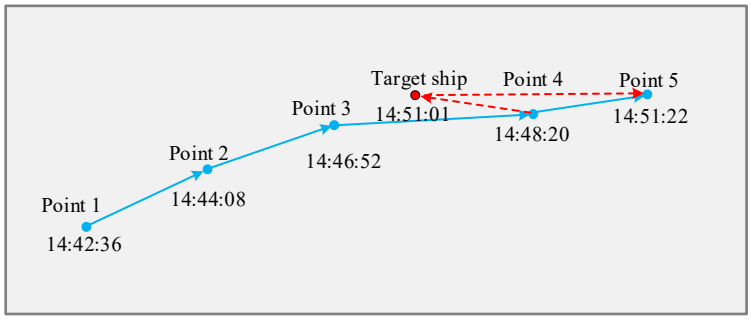

Figure 4. Mismatching of point–track based purely on spatial feature similarity.

This study uses the directional consistency of the sailing ship to describe the similarities in temporal features. The two blue dots, Points 4 and 5, represent continuous points on the ship track, and the red dot is the target point, as shown in Figure 5. The target point (ship) and two trajectory points form two vectors: $\overrightarrow{P_4T}$ and $\overrightarrow{TP_5}$. If the target point is connected to the track, the cosine of the angle formed by the two vectors can be used to assess the consistency of the sailing ship. If the cosine value is positive, the direction is consistent; otherwise, it is inconsistent.

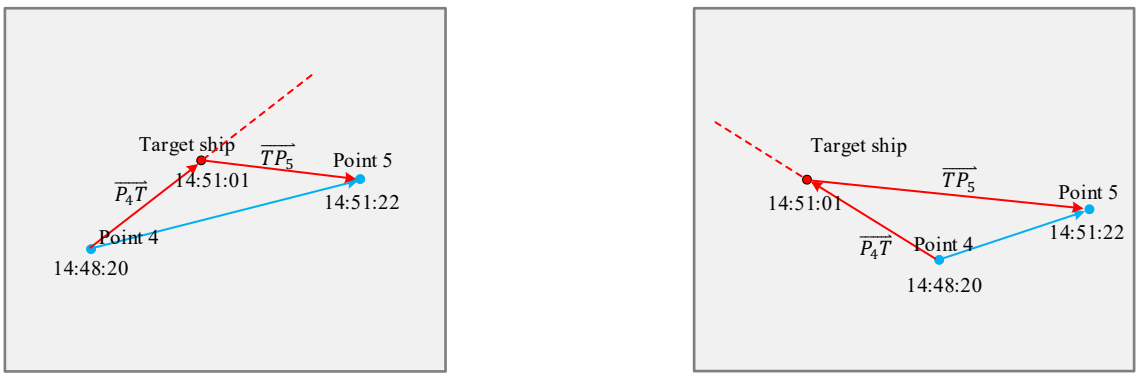

Figure 5. Direction consistency assessment based on vector cosine. (**a**) and (**b**) are two cases of the directional consistency of the sailing ship.

To calculate the time feature similarity quantitatively, the two closest points *pa* and *pb* in the ship track to the target point *tp* were first extracted and sorted by timestamp. The normalized time feature similarity *TFS* was then obtained using Equation (4):

$$TFS = \frac{1 + \frac{(x_{pa}-x_{tp})\times(x_{pb}-x_{pa})+(y_{pa}-y_{tp})\times(y_{pb}-y_{pa})}{\sqrt{(x_{pa}-x_{tp})^2+(y_{pa}-y_{tp})^2}\times\sqrt{(x_{pb}-x_{pa})^2+(y_{pb}-y_{pa})^2}}}{2} \quad (4)$$

where (x_{pa}, y_{pa}), (x_{pb}, y_{pb}), and (x_{tp}, y_{tp}) are the individual members of the tuples and can be considered as the longitude and latitude of points pa, pb, and tp.

4.1.3. Course Feature Similarity

Course feature similarity evaluates the course consistency between the target point and ship track. It is essential to ensure consistency over the ground in the movement of the target point relative to the ship track, as the target point in the cross-movement direction and the ship trajectory also have high spatial and temporal similarities. In Figure 6, the blue polyline denotes the ship track and the red point denotes the ship target point. Although the target point and ship trajectory are quite close in both space and time, the course of the target point, which assumes true north to be at 0°, will have an impact on the point–track matching result. Although 0 and 150° can essentially be ruled out, the target point is better matched with the track when its course value is between 60° and 90°.

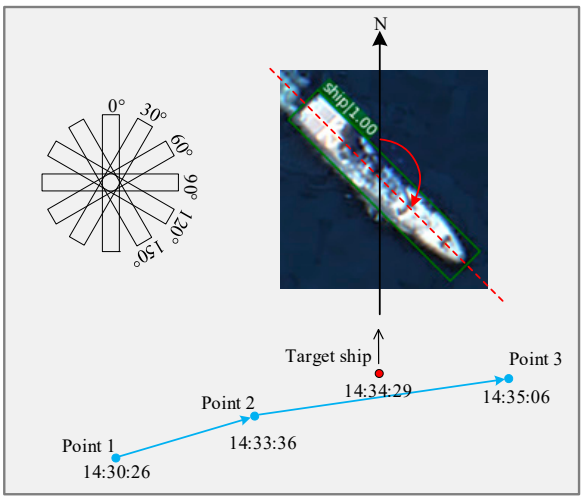

Figure 6. The importance of course feature similarity.

This study measured the course feature similarity by calculating the cosine value of the angle between the course of the target point and the course of the ship track. Ship target recognition from RS images can yield a rectangular bounding box of the ship target that contains the four corner coordinates of the ship position. The four corner coordinates are sorted in ascending order according to the longitudinal value, and are denoted as $c1$, $c2$, $c3$, and $c4$. The long side of the rectangular bounding box of the ship target can then be determined by the larger value of the distance between $c1$ and $c2$ and the distance between $c1$ and $c3$. The direction of the long side of the ground is the course of the ship's target point.

To quantitatively calculate the course feature similarity, this study assumes that the long sides of the rectangular bounding box of the ship target are $c1$ and $c3$, and the two closest points in the ship track to the target point are $p2$ and $p3$. The angle between the two vectors was selected as the acute angle. The normalized course feature similarity CFS was then obtained using Equation (5):

$$CFS = \frac{1 + \frac{(x_{c3}-x_{c1})*(x_{p3}-x_{p2})+(y_{c3}-y_{c1})*(y_{p3}-y_{p2})}{\sqrt{(x_{c3}-x_{c1})^2+(y_{c3}-y_{c1})^2}*\sqrt{(x_{p3}-x_{p2})^2+(y_{p3}-y_{p2})^2}}}{2} \quad (5)$$

where (x_{c1}, y_{c1}), (x_{c3}, y_{c3}), (x_{p2}, y_{p2}), and (x_{p3}, y_{p3}) are the individual members of the tuples and can be considered as the longitude and latitude of points $c1$, $c3$, $p2$, and $p3$.

4.1.4. Attribute Feature Similarity

Attribute feature similarity is the assessment of ship size consistency between the ship target points discovered from RS images and the ship size indicated in AIS data.

The attribute feature relies on previous knowledge discovered from AIS data. To increase the matching accuracy, the rectangular bounding box of the ship discovered using object recognition can be used to determine its size. After considering the acceptable error, the trajectory to be matched can be dismissed based on the attribute-matching result, because the attribute feature is an objective and truthful indicator. The attribute feature similarity AFS is represented mathematically as follows in Equation (6):

$$AFS = \begin{cases} e^{-(\frac{|width-W|}{W}+\frac{|length-H|}{H})}, e^{-(\frac{|width-W|}{W}+\frac{|length-H|}{H})} \geq \varepsilon \\ 0 \qquad\qquad\qquad\qquad , e^{-(\frac{|width-W|}{W}+\frac{|length-H|}{H})} < \varepsilon \end{cases} \tag{6}$$

The AFS is normalized by the exponential function. H and W are determined by the bounding box of the ship, while *length* and *width* are determined by AIS data. The acceptable error is concretized as the threshold ε. In this study, if the width of the bounding box did not exceed one-half of the true value and the length did not exceed one-fifth of the true value, it was considered a successful match, so the threshold was set to 0.5 after exponential operations.

The precision of the bounding box is critical for estimating attribute feature similarity. However, the size of a ship is often overestimated in RS images when it resembles the wake or waves around it. Figure 7 depicts the scenarios in which the bounding box of the ship target contains wakes in the sailing states at low, medium, and high speeds. While the length and width of the bounding box warp to variable degrees when traveling at high speeds, the wake has little impact on the size of the ship at low and medium speeds. The severity of the length distortion increases with speed.

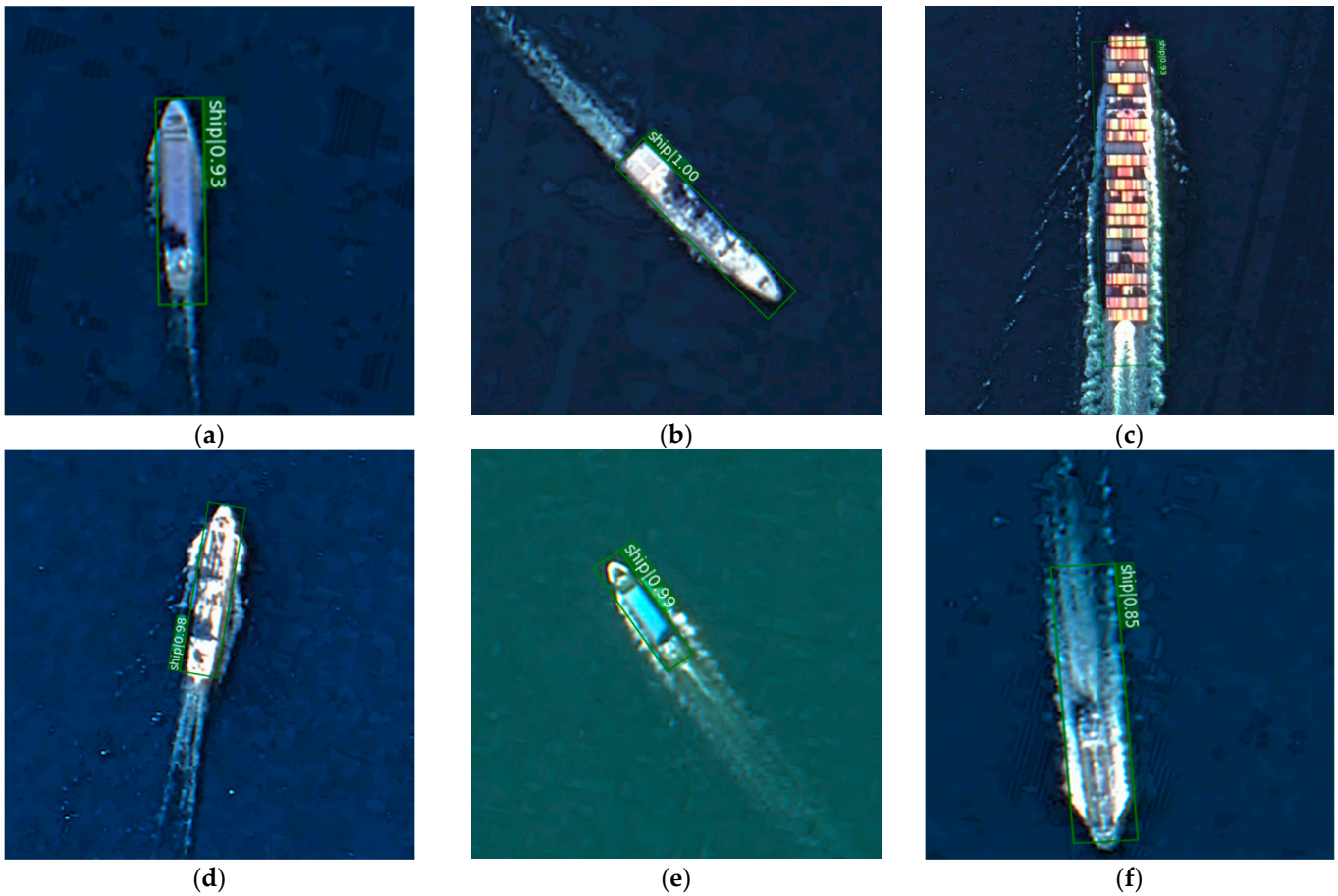

(**a**) (**b**) (**c**)

(**d**) (**e**) (**f**)

Figure 7. Effects of wake on bounding box in different operating states: (**a**,**d**) are low speed, (**b**,**e**) are medium speed, and (**c**,**f**) are high speed.

As a result, this study adjusts the confidence of the bounding box length and width to correct the distortion of the target recognition findings. It considers how the trajectory speed in the AIS data affects confidence. The AFS should add the ship's speed during calculation with the correction factors α_W and α_H:

$$A_a = e^{-(\alpha_W \frac{|width-W|}{W} + \alpha_H \frac{|length-H|}{H})} \tag{7}$$

$$AFS = \begin{cases} A_a, A_a \geq \varepsilon \\ 0, \ A_a < \varepsilon \end{cases} \tag{8}$$

The correction factors α_W and α_H are constructed by a piecewise function to describe the relationship with ship speed. Generally, when the ship speed is faster, the resulting wake is longer, and the bounding box score is lower, so the bounding box score is used as an evaluation index. Based on the experimental result and expert experience, we designed the following classification function. If the speed is less than 10 kn, the confidence of the length and width remains the same with no correction. When the speed is 10 to 15 kn, the factor of the long axis α_H is reduced to the score, and α_W remains unchanged. A speed greater than 15 kn means the ship is driving at high speed, and the white waves generated around the ship may also be recognized at this time. Thus, the value of the correction factor is further reduced, as calculated in Equation (9):

$$f(\alpha, v) = \begin{cases} \alpha_W = \alpha_H = 1, \ 0 < v \leq 10kn; \\ \alpha_W = 1, \alpha_H = score, 10 < v \leq 15; \\ \alpha_W = \frac{v}{v_{max}}, \alpha_H = \frac{v}{v_{max}} score, 15 \leq v \leq v_{max} \end{cases} \tag{9}$$

4.2. Fuzzy Point–Track Association

Traditional methods that rely on calculating spatiotemporal distances often face challenges in densely populated areas, where small differences in distances can significantly affect the matching results and reduce matching accuracy. By employing fuzzy mathematics, similarity values can be fuzzified, allowing for a more effective handling of uncertainty. This approach enhances robustness in ship trajectory matching [25]. In this section, the interval type-2 fuzzy system (IT2FS) [15] is used to assess the fuzzy point–track association. The IT2FS can implement a weighted average at the semantic level and produce precise results from fuzzy semantic description data. Three processes are involved in the fuzzy association of points and tracks: multi-dimensional feature similarity fuzzification [23], fuzzy association rule generation, and fuzzy inference [26]. The membership functions of the IT2FS are all Gaussian membership functions with the uncertain standard deviation IT2FS_Gaussian_UncertStd [27]. The most common center-of-sets price reducer and the Nie–Tan algorithm [28] are selected for price reduction and defuzzification.

4.2.1. Interval Type-2 Fuzzy Sets

An interval type-2 fuzzy set, denoted as $\widetilde{F}$, is characterized by a type-2 membership function $\varphi_{\widetilde{F}}(x, u) = 1$ as:

$$\widetilde{F} = \left\{ \left((x, u), \varphi_{\widetilde{F}}(x, u) \right) \mid \forall x \in X, \forall u \in G_x \sim N\left(\mu, \sigma^2\right) \right\} \tag{10}$$

where x is a membership value with the domain X; u is a membership value belonging to the membership function G_x, and G_x is a Gaussian distribution with the mean μ and the variance σ^2.

An IT2FS is defined by its lower membership function (LMF) and upper membership function (UMF), and the area between all upper and lower membership functions constitutes the footprint of uncertainty (FOU) [29]:

$$\text{UMF} = \left\{ ((x, u_x)) \mid \forall x \in X, \forall u \in G_x \sim N\left(\mu_u, \sigma_u^2\right) \right\} \tag{11}$$

$$\mathrm{LMF} = \left\{ ((x, l_x)) \mid \forall x \in X, \forall l \in G_x \sim N\left(\mu_l, \sigma_l^2\right) \right\} \tag{12}$$

$$FOU = \bigcup_{x \in X} x \times [l_x,\ u_x] \tag{13}$$

where x is a membership value with the domain X; u_x is the UMF belonging to a Gaussian distribution G_x with the mean μ_u and the variance σ_u^2; and l_x is the UMF belonging to a Gaussian distribution G_x with the mean μ_l and the variance σ_l^2.

4.2.2. Multi-Dimensional Feature Similarity Fuzzification

To achieve variable fuzzification, multi-dimensional feature similarities with precise values in the point–track similarity model were mapped to a fuzzy set defined by the domain of fuzzy reasoning [13].

Spatiotemporal fuzzy similarity A_p: This combines the spatial and temporal feature similarities. Specifically, it refers to the distance between the location coordinates p_j (latitude and longitude) of the ship target in the RS image and the spatial position p_i^t of the track point obtained via interpolation at time t. Distance is measured by the Euclidean distance in meters as calculated in Equation (14):

$$A_p(p_i^t, p_j) = \sqrt{(p_i^t.lon_i - p_j.lon_j)^2 + (p_i^t.lat_i - p_j.lat_j)^2} \tag{14}$$

where lon_i and lat_i are the longitude and latitude of the track point, and lon_j and lat_j are the longitude and latitude of the ship target point, respectively.

Since "near and far" are common vague terms used to describe the magnitude of distance, the fuzzy similarity A_p can be defined as Near, Medium, or Far. As shown in Figure 8, the value range of the Euclidean distance is restricted to [0, 3000] according to the interpolation results. The maximum distance is determined based on the interpolation results of the trajectory. Due to fluctuations in trajectory data, the calculated distance may have exceeded 2500 m in the preliminary experiments. Therefore, 3000 was chosen as the maximum limit. When the Euclidean distance exceeded 3000 m, it was determined to be irrelevant without the requirement for fuzzy inference. Here, the membership function of spatiotemporal fuzzy similarity adopts a Gaussian membership degree. Since the existence of fluctuations in trajectory data, it is not comprehensive to simply judge whether it is far or near based on the distance, so the membership functions of each variable were designed in an overlapping manner. The standard deviation center and standard deviation spread of the variables Near and Far were 750 and 100, and the standard deviation center and standard deviation spread of the variable Medium were 375 and 100. The value range of the membership functions was normalized to [0, 1].

Course fuzzy similarity A_c: A_c is defined as Close or Differ to describe the difference in the course. As seen in Figure 9, since course feature similarity is the cosine value of the angle between the course of the target point and the course of the ship track, its value range is [0, 1]. Based on the calculated cosine value, the course similarity can be transferred to the fuzzy set using an overlapping Gaussian membership function, and the value range of A_c is also [0, 1], since the smaller the angle, the smaller the deviation of the heading, the higher the cosine value and A_c. This study adjusted the center and spread of the standard deviation to ensure the larger cosine value fell within the range of Close. Therefore, the standard deviation center and standard deviation spread of the variable Close were 0.125 and 0.05, and the standard deviation center and standard deviation spread of the variable Differ were 0.3 and 0.05.

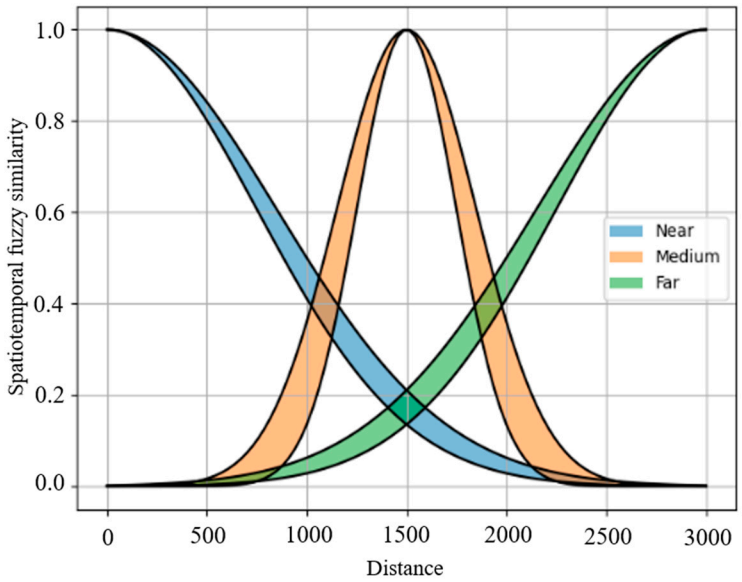

Figure 8. Membership function of spatiotemporal fuzzy similarity.

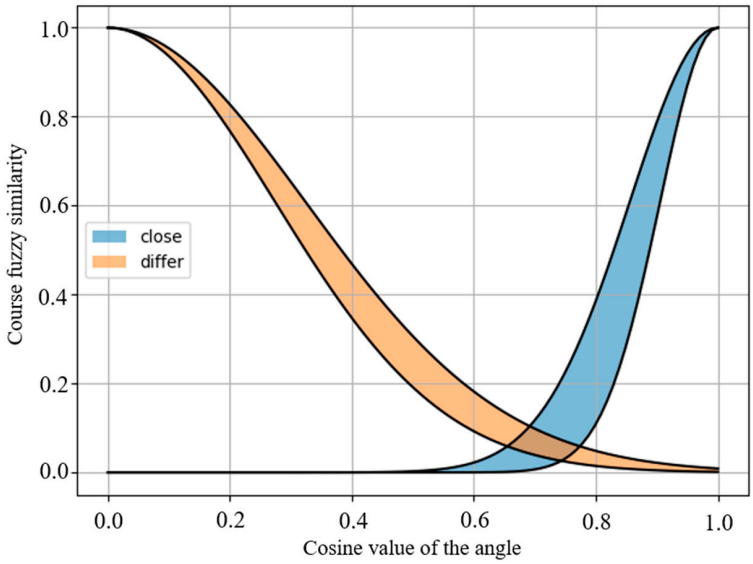

Figure 9. Membership function of course fuzzy similarity.

Attribute fuzzy similarity A_a: A_a is defined as Consistent or Inconsistent. In Section 4.1.4, the attribute feature similarity (AFS) is expressed by an exponential function with the domain [0, 1]. As seen in Figure 10, according to the calculated exponential value, AFS can be projected to A_a's membership function. The bigger the exponential value, the higher the AFS, and the larger the A_a. Then, it can be further transferred into the fuzzy set Consistent and Inconsistent. Similar to the course fuzzy similarity, the standard deviation center of the variable Consistent was further adjusted because the confidence of attribute fuzzy similarity was higher. The standard deviation center and standard deviation spread of the variable Consistent were 0.1 and 0.05, and the standard deviation center and standard deviation spread of the variable Inconsistent were 0.3 and 0.05.

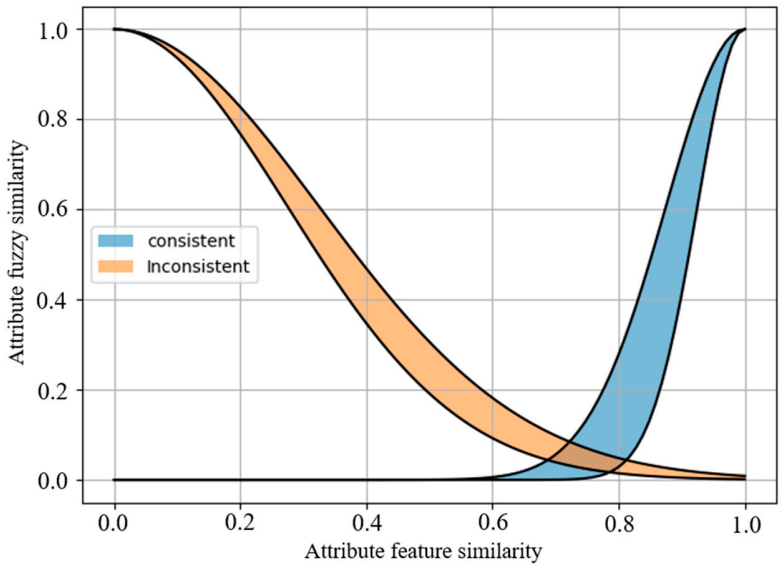

Figure 10. Membership function of attribute fuzzy similarity.

Output: feature correlation degree A_s: A_s describes the point–track association degree. It combines spatiotemporal fuzzy similarity, course fuzzy similarity, and attribute fuzzy similarity, so the value range is [0, 3], and the value range of the membership function is normalized to [0, 1]. As shown in Figure 11, the fuzzy set of A_s was set as Low, Medium, and High. The feature correlation degree is the result of fuzzy calculation, Low and High correlation degrees can be directly divided according to the median value without considering fluctuations as in Figure 8. So, the membership function has no intersection between Low and High. All the variables' standard deviation center and standard deviation spread were set as 0.4 and 0.15. In intuitive cognition, when the sum of the three similarities is lower than 0.75, it is considered that the point–track association degree is low, but in this study, A_s was obtained based on fuzzy association rules rather than by adding the three values directly.

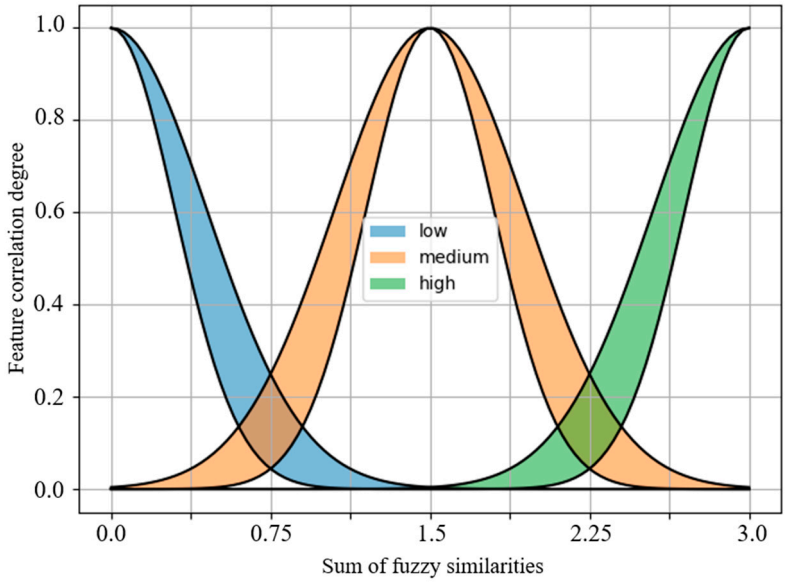

Figure 11. Membership function of feature correlation degree.

4.2.3. Fuzzy Association Rules for Point-Track Matching

The fuzzy inference model uses fuzzy semantic rules to describe inference relationships [30]. Based on the fuzzy processing of the input and output variables, this study uses the common-sense reasoning of the intuitive empirical method to construct fuzzy rules for the relationship between points and traces. Because the spatiotemporal fuzzy similarity A_p and course fuzzy similarity A_c are applicable to any ship trajectory and target ship in the RS image, and the attribute fuzzy similarity A_a may have missing data, the association can be divided into two steps. The first step is to correlate the fuzzy similarity of spatiotemporal and course features to obtain the basic correlation A'_s. In the second step, based on the basic correlation A'_s, the attribute of fuzzy similarity is added for further association, and the point–track association is ultimately obtained as the degree A_s.

In the first step, the fuzzy inference rule for basic associations is described as follows:

$$\begin{gathered} A'_s = \text{Low}, if\ A_c\ is\ differ\ or\ A_p\ is\ far \\ A'_s = \text{Medium}, if\ A_c\ is\ close\ and\ A_p\ is\ \text{medium} \\ A'_s = \text{High},\ if\ A_c\ is\ close\ and\ A_p\ is\ near \end{gathered} \tag{15}$$

where A_p is the spatiotemporal fuzzy similarity and A_c is the course fuzzy similarity. The fuzzy inference rules consider the basic correlation A'_s between two fuzzy similarities in different states.

In the second step, by combining the obtained A'_s with the attribute of fuzzy similarity A_a, the fuzzy inference rule of the point–track correlation degree is described as follows:

$$\begin{gathered} A_s = \text{Low},\ if A'_s\ is\ Low \\ A_s = \text{Low},\ if A'_s\ is\ Medium\ and\ A_a\ is\ \text{inconsistent} \\ A_s = \text{Medium},\ if A'_s\ is\ High\ and\ A_a\ is\ \text{inconsistent} \\ A_s = \text{High},\ if A'_s\ is\ Medium\ and\ A_a\ is\ \text{consistent} \\ A_s = \text{High}, if\ A'_s\ is\ High\ and\ A_a\ is\ \text{consistent} \end{gathered} \tag{16}$$

where A_s is the point–track correlation degree and its value relates to the different states of the basic correlation A'_s and the attribute fuzzy similarity A_a.

4.2.4. Spatiotemporal Association of Multi-Source Ship Locations

To achieve the fuzzification of variables, similarities with precise values in the point–track similarity model were mapped to the fuzzy set defined by the discourse universe of fuzzy reasoning. Assuming that the ship target set extracted from the RS image is $S(t) = [S_1, \ldots, S_m]$, m is the number of ships extracted from the current image, and t is the RS image capture time. The trajectory set in the spatial extent of the image is $T(t) = [T_1, \ldots, T_n]$, with n being the number of trajectories queried around the image capture time. The spatiotemporal association of multi-source ship locations individually matches the extracted ship targets with the queried trajectories. The matching process has three steps, as detailed below.

Step 1: Calculate the fuzzy correlation degree matrix. For the ship trajectory T_i and ship position S_j, the feature correlation degree $A_s^{i,j}$ is calculated by applying the point–trace

correlation fuzzy inference module above. For m ship targets in $S(t)$ and n tracks in the trajectory set $T(t)$, the fuzzy correlation degree matrix $A_s(t)$ can be calculated as:

$$A_s(t) = \begin{bmatrix} A_s^{1,1} & \cdots & A_s^{1,n} \\ \vdots & \ddots & \vdots \\ A_s^{m,1} & \cdots & A_s^{m,n} \end{bmatrix} \tag{17}$$

Step 2: Generate the cost matrix $G(t)$. In $A_s(t)$, the value range of $A_s^{i,j}$ is [0, 3]. The larger the value, the higher the similarity. When the value is lower than the threshold σ (σ = 1 in this study), it can be directly considered to have no related relationship, as follows:

$$A_s^{i,j} = 0, \text{ if} A_s^{i,j} < \sigma \tag{18}$$

If all the elements of a row are 0, the image ship corresponding to this row does not have a correct matching track, so it is removed from the matrix to reduce matching operations. After normalization, for m targets and n tracks after filtering, the cost matrix $G(t)$ is defined as:

$$G(t) = 1 - A_s(t) \tag{19}$$

In $G(t)$, the value range is still [0, 1]; a smaller value indicates a lower cost and higher matching degree.

Step 3: Match the point and track. According to the results of the fuzzy correlation degree matrix $A_s^{i,j}$, the degree of correlation between the same ship and multiple trajectories may be greater than the threshold σ, and the point–track matching problem can be converted into a matching problem for weighted bipartite graphs. The Hungarian algorithm [31] is used to determine the optimal match.

For m ship targets in $S(t)$ and n tracks in $T(t)$, assume that S_1 can match with T_1 and T_2, and $A_s^{1,1} > A_s^{1,2}$. First, the algorithm matches T_1 with S_1 according to the principle of the highest degree of correlation, and $S_1 \to T_1$ is called the matching edge. Then, turning to finding the matching edge of S_2, assuming that S_2 can only match with T_1, then $S_2 \to T_1 \to S_1 \to T_2$ is called an augmented path. The augmented path starts from an unmatched ship target (S_2), passes through a non-matching edge ($S_2 \to T_1$), matching edge ($T_1 \to S_1$), and non-matching edge ($S_1 \to T_2$), and ends at another unmatched track (T_2). The core of the Hungarian algorithm is to find all augmented paths of each ship target until there is no new augmented path. Algorithm 1 presents the recursive process for determining the augmenting path.

Algorithm 1. Hungarian algorithm

Input : A $m \times$
n cos t matrix $G(t)$, including m ship targets in $S(t)$ and n tracks in trajectory set $T(t)$.
Output: The matching pairs between ship trajectory sets and ship targets

```
while (the ship target S_i have a matching track T_j) do
    if (the track T_j is not in the augmenting path) then
        add T_j into the augmenting path;
        if (T_j is a non −
matching point or it's able to find another augmenting path starting from T_j) then
            change the matching edge as S_i → T_j;
            return true;
        end if
    end if
    return false
end while
```

4.3. Ship Detection and Evaluation Indicators

The application of the object detection models can help easily obtain the position and bounding box of the ship in RS images, and then apply these to achieve similarity extraction as in Section 4.1. Deep learning techniques, such as oriented R-CNN, have proven to be effective for ship detection. We performed detection based on a pretrained model trained on the HRSC2016 dataset [32]. The original GF1 and GF2 images were cropped into 1024 × 1024 patches for detection. The prediction bounding boxes of the ship were expressed in terms of confidence, and we retained the prediction results with confidence larger than 0.8 for filtering. At this time, the intersection over union (IoU) of the model result is the highest, that is, the coincidence between the detection result and the ship position is optimal. Figure 12 presents the results of ship detection using the oriented R-CNN algorithm.

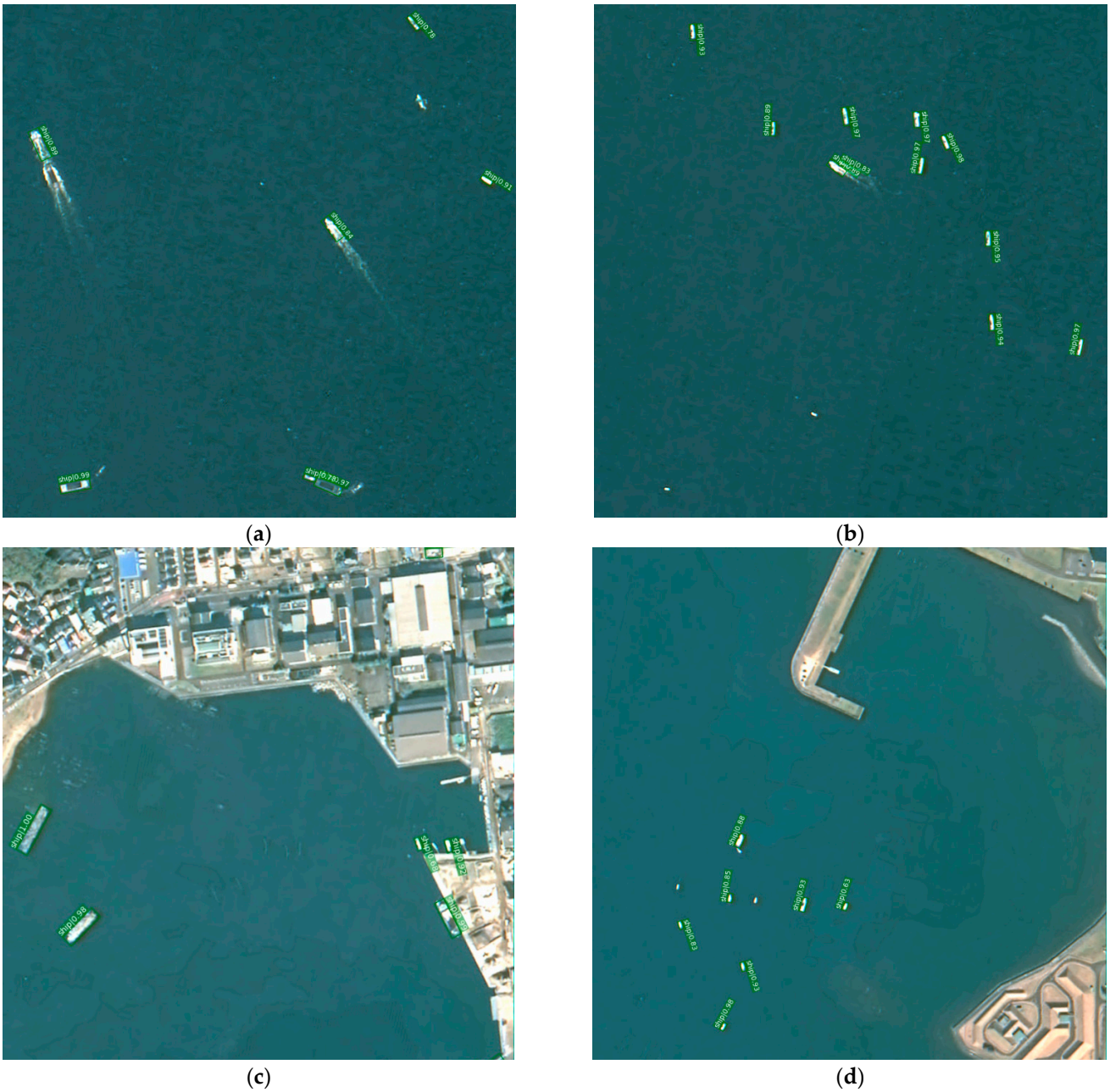

Figure 12. Ship detection results using the oriented R-CNN algorithm. (**a**,**b**) are examples from GF1 images, and (**c**,**d**) are examples from GF2 images.

We first outline a method for evaluating trajectory matching results. As shown in Figure 13, for each ship to be verified, we obtained its bounding box from the RS image and measured the length and width using ArcGIS. Based on the trajectory matching results, we retrieved the MMSI number, allowing us to query ship size information from the archives. If the difference between the two size measurements was below the threshold of 3 m, the matching result was deemed correct. In this study, manual visual interpretation was employed to verify the matching results between ship entities and AIS trajectories, yielding 31 and 37 correctly matched entities in GF1 and GF2 images, respectively.

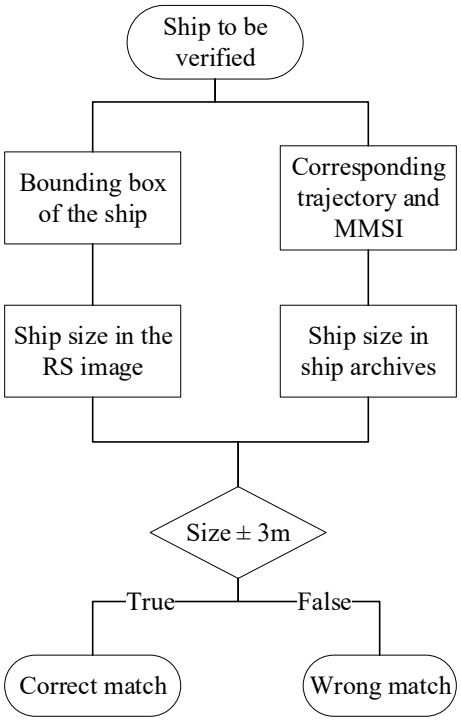

Figure 13. Method for judging the results of ship matching.

5. Analysis of Experimental Results

5.1. FOU Evaluation

The results of the model were determined by UMF and LMF. FOU characterizes the uncertain information of fuzzy sets. We evaluated different FOU sizes by adjusting the range of $[l_x, u_x]$ in formula 13 to obtain the optimal parameter results. As shown in Figure 14, (a–f) are membership functions at different FOU sizes, and (g) is the corresponding model result. We used the F1 value as a comprehensive evaluation indicator. Since the resolutions of GF1 and GF2 were different, we counted the matching results for GF1 and GF2. The FOU size "±5%, ±10%, ±20%, ±30%, ±40%, ±50%" inferred the F1 scores of 0.6957, 0.6970, 0.7188, 0.7188, 0.7302, and 0.7213, respectively, in GF1 images, and 0.8049, 0.8571, 0.8533, 0.8611, 0.8732, and 0.8732, respectively, in GF2 images. The model achieved the best result when the FOU size was ±40%.

5.2. Accuracy Evaluation

We experimented and verified the point–track similarity matching model using GF1 and GF2 images. Table 1 presents the experimental results for GF1 and GF2 within the correlation degree range of 0.4 to 0.8, as extremes may suppress potential matches.

As shown in Table 1, in GF1 images, the F1 score remains at a high level of 0.7302 when the correlation degree was 0.5. The F1 score decreases sharply at higher thresholds. According to the fuzzy association rules, if the feature similarity results fall within the medium range, it is considered a true match. Under these conditions, the requirements for point–trace matching are relatively low, resulting in higher accuracy and recall. As

the threshold increases, the fuzzy correlation degree becomes higher, leading to stricter matching criteria. Consequently, the number of successful matches in the medium range decreases, resulting in a sharp drop in recall, while accuracy remains largely unchanged. These findings indicate that a high fuzzy correlation degree can effectively ensure the correctness of matching results.

In Table 1, it can be seen that for the GF2 images, the matching model guarantees a higher F1 score of 0.9189 when the correlation degree is set to 0.5. In the case of low resolution, the ship sizes in the GF1 images are less than half that in the GF2 images (2 m for GF1 and 0.8 m for GF2). This reduced size makes it challenging to identify ships under sailing conditions. In contrast, stationary ships, such as those moored at sea or in ports, are easier to detect. During manual verification, nearly half of the entities in the detection results of the GF1 images were ships docked in ports. The proximity to shore contributes to more false detections, while the AIS track points for moored ships can be affected by waves and positioning inaccuracies, leading to irregular point clusters that complicate course feature utilization. Consequently, these factors contribute to poor matching results. With improved resolution in GF2 images, the recognition of ships is markedly enhanced, making it easier to identify vessels in a sailing state. As a result, the point–trace matching performance in GF2 significantly outperforms that of GF1.

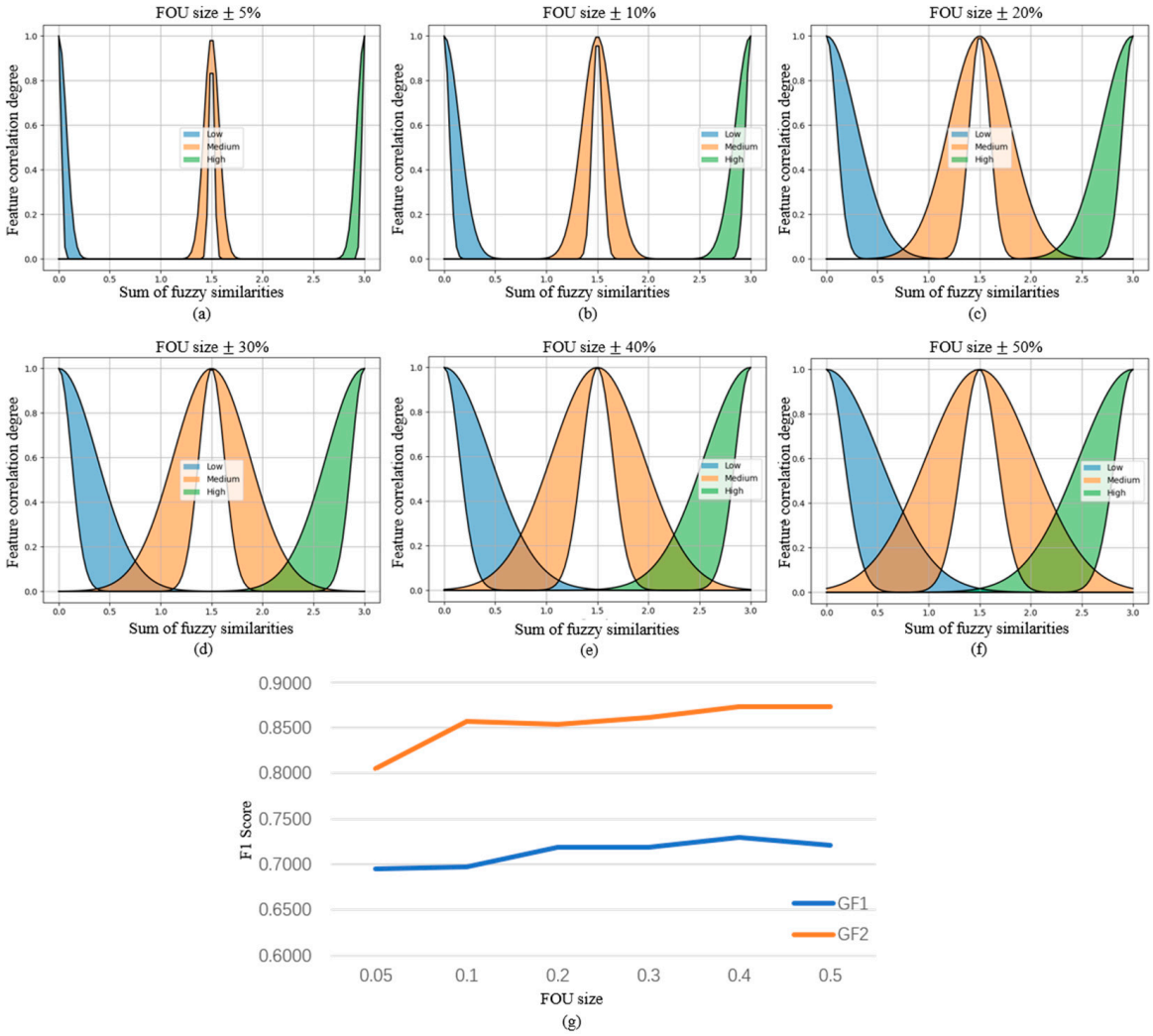

Figure 14. Membership functions and F1 scores computed by different FOU sizes. (**a**–**f**) are membership functions at different FOU sizes, and (**g**) is the corresponding model result.

Table 1. Matching results in Gaofen-1 and Gaofen-2 images among different correlation degrees. The maximum value is in bold.

Dataset	Correlation Degree	Total Match	True Match	Accuracy	Recall	F1
GF1	0.4	32	23	0.7188	0.7419	0.7302
	0.5	32	23	0.7188	0.7419	**0.7302**
	0.6	19	14	0.7368	0.4516	0.5600
	0.7	19	14	0.7368	0.4516	0.5600
	0.8	11	8	0.7273	0.2581	0.3810
GF2	0.4	37	34	0.9189	0.9189	0.9189
	0.5	37	34	0.9189	0.9189	**0.9189**
	0.6	36	33	0.9167	0.8919	0.9041
	0.7	36	33	0.9167	0.8919	0.9041
	0.8	33	32	0.9697	0.8649	0.9143

Figure 15 shows the matching results obtained using the proposed model. The numbers are the MMSI numbers of the corresponding ships. For example, the MMSI number of the ship matched by the trajectory corresponding to the yellow line in (a) in the figure is 431,000,841.

(**a**) (**b**)

Figure 15. Example of matching result using the proposed model. (**a**,**b**) are matching examples in this study, each polyline in the figure is drawn according to the AIS record, and the number next to it is the corresponding MMSI number.

5.3. Performance Comparison

In this study, the ablation and compared experiments were designed to verify the effectiveness of the proposed method. We compared the point–track correlation results using multi-feature combinations on images of different resolutions (GF1 and GF2). The ablation experiment was divided into three groups, and the parameters of the model were kept consistent or default. The first group was the spatiotemporal fuzzy similarity with the combination of time and space. The second group was the spatiotemporal fuzzy similarity and course fuzzy similarity. The third group was the proposed method with all the fuzzy similarities. The comparison experiment was performed by multi-factor fuzzy comprehensive decision-making (MFCD) and classification and regression trees (CART); the correlation degree was set as 0.5. Both MFCD and CART use multi-dimensional feature similarities. To apply the CART algorithm, we constructed 81 ship-matching samples for training according to feature similarities following the organizational format of the Iris dataset. Tables 2 and 3 show the accuracy and recall of matching for the GF1 and GF2 images.

Table 2. Matching results in Gaofen-1 images. The maximum value is in bold.

Algorithm	Total Match	True Match	Accuracy	Recall	F1
Spatiotemporal	15	12	0.8000	0.3871	0.5217
Spatiotemporal + Course	20	13	0.6500	0.4194	0.5098
MFCD	30	20	0.6667	0.6452	0.6557
CART	30	18	0.6000	0.5806	0.5902
Proposed method	32	23	0.7188	0.7419	**0.7302**

Table 3. Matching results in Gaofen-2 images. The maximum value is in bold.

Algorithm	Total Match	True Match	Accuracy	Recall	F1
Spatiotemporal	35	25	0.7143	0.6757	0.6944
Spatiotemporal + Course	41	32	0.7805	0.8649	0.8205
MFCD	30	24	0.8000	0.6486	0.7164
CART	38	32	0.8421	0.8649	0.8533
Proposed method	37	34	0.9189	0.9189	**0.9189**

Table 2 lists the ablation and comparison experimental results for the GF1 images. The proposed method achieves the best F1 score of 0.7302, which is greater than those of MFCD and CART. At the same time, the performance of the first two groups is relatively poor. When only spatiotemporal fuzzy similarity is applied, the accuracy of point–trace matching reaches a peak of 0.8; however, the recall rate is very low, indicating that while spatiotemporal positioning can serve as a foundation for matching, its effectiveness is limited. Adding course fuzzy similarity does not significantly improve accuracy or recall, which aligns with previous observations about the low resolution of GF1 images, where most ships are docked near the port, making course features challenging to utilize. In contrast, the proposed method, which incorporates attribute fuzzy similarity, enhances the confidence of the matching results. This addition helps to compensate for the limitations posed by low resolution and the difficulties in using course features, leading to more reliable matching outcomes.

Table 3 shows the ablation experiment results and comparison experiment results for GF2 images. As the number of features increases, the accuracy of the proposed model also improves, with the F1 score reaching 0.9189 when all features are utilized. Notably, the highest recall rate is achieved with the second feature combination, attributed to the greater number of ships in a sailing state in the GF2 images. Unlike GF1, the course feature in GF2 is more accurate and effectively utilized. However, the recognition of sailing ships can be influenced by wakes, which affect attribute information extraction as discussed in Section 4.1.4. Although some corrections are applied, errors persist, leading to a slight decrease in recall when all similarities are employed. Nevertheless, the inclusion of attribute similarity significantly filters out incorrect matches, resulting in a 13% increase in accuracy.

In general, the incorporation of feature similarities significantly enhances point–track matching results. The proposed method achieves optimal performance with all fuzzy similarities across different resolutions, demonstrating that a higher image resolution correlates with improved outcomes. This underscores that the proposed model, based on multi-feature combinations, effectively facilitates point–track associations.

5.4. Efficiency Comparison

We evaluated the efficiency of the methods in both ablation and comparative experiments by measuring their running times across different resolutions. The average time consumed by each method for all GF images is summarized in Table 4. It is important to note that this experiment utilized the ClickHouse database to retrieve AIS data during execution, requiring the traversal of all tracks within the image range, with a time span of 5 min before and after the image capture. Consequently, running time is proportional to the number of trajectories; more tracks lead to increased running times. Thus, the basic time

consumption for using only spatiotemporal fuzzy similarity is notably high. As the number of similarities increases, the running time of the proposed model also rises gradually, but the increase is relatively small. This suggests that adding similarity features does not significantly escalate the computational burden. However, the time consumption of the proposed method is longer than that of the multi-factor fuzzy comprehensive decision-making (MFCD) method, indicating that while the use of IT2FS may sacrifice some efficiency, it results in higher matching accuracy.

Table 4. Matching results in Gaofen images. The minimum value is in bold.

Algorithm \ Images / Time(s)	GF1	GF2
Spatiotemporal	326.5	824.7
Spatiotemporal + Course	370.5	863.3
Proposed method	381	895
MFCD	382.5	**627**

6. Conclusions

There are more specific areas, such as port approaches, critical infrastructure, and fishing areas, where AIS data alone are not reliable and other methods for ship observation and detection have to be applied. Matching automatic identification system data and remote sensing images is one of the opportunities for interested parties to perform their job properly. This study introduces a multi-feature-based point–track association method that integrates AIS trajectory data with RS images, utilizing the Interval Type-2 Fuzzy Sets (IT2FS) approach for fuzzy point–track association. The experiments conducted using the GF1 and GF2 images demonstrate that while the proposed method sacrifices some efficiency, it achieves optimal performance, with F1 scores of 0.7302 for GF1 and 0.9189 for GF2, indicating better association results at higher resolutions. This study's contributions include the comprehensive utilization of four characteristics—space, time, course, and attribute—to extract relationships between ships and their trajectories, as well as the development of a similarity modeling method for multi-dimensional features. Additionally, a feature fuzzification method and fuzzy matching rules were designed, with fuzzy mathematics employed to construct the relationship between ambiguity and similarity. Ultimately, point–track matching is accomplished using the Hungarian algorithm.

However, the proposed method has certain limitations. First, its application scenario is primarily suited for ship trajectory matching in the sailing state. In the mooring state, course features are less effectively utilized, which can restrict the model's accuracy. Secondly, the accuracy of the attribute features depends on the ship recognition results. Higher model recognition accuracy leads to better attribute feature accuracy. Additionally, the speed threshold is determined not by the algorithm itself but through empirical experiments and expert insights. Therefore, in future research, we will distinguish and extract ship features under sailing and berthing states to improve the model's generalization, and consider realizing the automatic extraction of ship speed based on deep learning technology to better deal with these distortions.

Author Contributions: Conceptualization, W.G.; Data curation, M.Z.; Funding acquisition, W.G. and L.H.; Methodology, Y.L.; Resources, P.v.G.; Visualization, K.L.; Writing—original draft, R.W.; Writing—review and editing, L.H. All authors have read and agreed to the published version of the manuscript.

Funding: This research was funded by the National Natural Science Foundation of China, grant number 42071431, and the Research Program of Sanya City, grant number No. 2022KJCX36.

Institutional Review Board Statement: Not applicable.

Informed Consent Statement: Not applicable.

Data Availability Statement: Data are contained within the article.

Conflicts of Interest: The authors declare no conflicts of interest.

References

1. Han, X.; Fu, S.; Han, J. Detection and Tracking of Low-Frame-Rate Water Surface Dynamic Multi-Target Based on the YOLOv7-DeepSORT Fusion Algorithm. *J. Mar. Sci. Eng.* **2024**, *12*, 1528. [CrossRef]
2. Zhang, C.; Zhang, X.; Gao, G.; Lang, H.; Liu, G.; Cao, C.; Song, Y.; Guan, Y.; Dai, Y. Development and Application of Ship Detection and Classification Datasets: A Review. *IEEE Geosci. Remote Sens. Mag.* **2024**, 2–36. [CrossRef]
3. Chen, X.; Ma, D.; Liu, R.W. Application of Artificial Intelligence in Maritime Transportation. *J. Mar. Sci. Eng.* **2024**, *12*, 439. [CrossRef]
4. Chen, X.; Wu, H.; Han, B.; Liu, W.; Montewka, J.; Liu, R.W. Orientation-Aware Ship Detection via a Rotation Feature Decoupling Supported Deep Learning Approach. *Eng. Appl. Artif. Intell.* **2023**, *125*, 106686. [CrossRef]
5. Xie, X.; Cheng, G.; Wang, J.; Yao, X.; Han, J. Oriented R-CNN for Object Detection. In Proceedings of the 2021 IEEE/CVF International Conference on Computer Vision (ICCV), Montreal, QC, Canada, 10–17 October 2021.
6. Thombre, S.; Zhao, Z.; Ramm-Schmidt, H.; Vallet García, J.M.; Malkamäki, T.; Nikolskiy, S.; Hammarberg, T.; Nuortie, H.; Bhuiyan, M.Z.H.; Särkkä, S.; et al. Sensors and AI Techniques for Situational Awareness in Autonomous Ships: A Review. *IEEE Trans. Intell. Transp. Syst.* **2022**, *23*, 64–83. [CrossRef]
7. Zhao, W.; Wang, D.; Gao, K.; Wu, J.; Cheng, X. Large-Scale Long-Term Prediction of Ship AIS Tracks via Linear Networks with a Look-Back Window Decomposition Scheme of Time Features. *J. Mar. Sci. Eng.* **2023**, *11*, 2132. [CrossRef]
8. Zhang, D.; Zhang, Y.; Zhang, C. Data Mining Approach for Automatic Ship-Route Design for Coastal Seas Using AIS Trajectory Clustering Analysis. *Ocean. Eng.* **2021**, *236*, 109535. [CrossRef]
9. Li, J.; Hong, D.; Gao, L.; Yao, J.; Zheng, K.; Zhang, B.; Chanussot, J. Deep Learning in Multimodal Remote Sensing Data Fusion: A Comprehensive Review. *Int. J. Appl. Earth Obs. Geoinf.* **2022**, *112*, 102926. [CrossRef]
10. Chen, M.; Zhang, L.; Deng, M.; Zhu, J. Marine Scene-Level Ship Matching Algorithm Based on Jilin-1 Data and AIS. In Proceedings of the 2023 IEEE 6th International Conference on Information Systems and Computer Aided Education (ICISCAE), Dalian, China, 23–25 September 2023; pp. 288–292.
11. Rodger, M.; Guida, R. Data Association Techniques for Near-Contemporaneous SAR and AIS Datasets from NovaSAR-1. In Proceedings of the IGARSS 2019—2019 IEEE International Geoscience and Remote Sensing Symposium, Yokohama, Japan, 28 July–2 August 2019; pp. 700–703.
12. Gong, X.; Huang, Z.; Wang, Y.; Wu, L.; Liu, Y. High-Performance Spatiotemporal Trajectory Matching across Heterogeneous Data Sources. *Future Gener. Comput. Syst.* **2020**, *105*, 148–161. [CrossRef]
13. Liu, C.; Xu, T.; Yao, T.; Deng, Z.; Liu, J. Data Association of AIS and Radar Based on Multi-Factor Fuzzy Judgment and Gray Correlation Grade. In *Communications, Signal Processing, and Systems*; Liang, Q., Mu, J., Jia, M., Wang, W., Feng, X., Zhang, B., Eds.; Springer: Singapore, 2019; pp. 1315–1322.
14. Jian, J.; Liu, L.; Zhang, Y.; Xu, K.; Yang, J. Optical Remote Sensing Ship Recognition and Classification Based on Improved YOLOv5. *Remote Sens.* **2023**, *15*, 4319. [CrossRef]
15. Mendel, J.M. General Type-2 Fuzzy Systems. In *Uncertain Rule-Based Fuzzy Systems*; Springer International Publishing: Cham, Switzerland, 2017; pp. 617–674. ISBN 978-3-319-51369-0.
16. Chaturvedi, S.K.; Yang, C.-S.; Ouchi, K.; Shanmugam, P. Ship Recognition by Integration of SAR and AIS. *J. Navig.* **2012**, *65*, 323–337. [CrossRef]
17. Ahmed, I.; Jun, M.; Ding, Y. A Spatio-Temporal Track Association Algorithm Based on Marine Vessel Automatic Identification System Data. *IEEE Trans. Intell. Transp. Syst.* **2022**, *23*, 20783–20797. [CrossRef]
18. Liu, Y.; Yao, L.; Xiong, W.; Zhou, Z. GF-4 Satellite and Automatic Identification System Data Fusion for Ship Tracking. *IEEE Geosci. Remote Sens. Lett.* **2019**, *16*, 281–285. [CrossRef]
19. Yang, Y.; Yang, F.; Sun, L.; Xiang, T.; Lv, P. Multi-Target Association Algorithm of AIS-Radar Tracks Using Graph Matching-Based Deep Neural Network. *Ocean. Eng.* **2022**, *266*, 112208. [CrossRef]
20. Kazimierski, W. Proposal of Neural Approach to Maritime Radar and Automatic Identification System Tracks Association. *IET Radar Sonar Navig.* **2017**, *11*, 729–735. [CrossRef]
21. Zou, H.; Sun, H.; Ji, K.; Du, C.; Lu, C. Multimodal Remote Sensing Data Fusion via Coherent Point Set Analysis. *IEEE Geosci. Remote Sens. Lett.* **2013**, *10*, 672–676. [CrossRef]
22. Liu, W.; Liu, Y.; Gunawan, B.A.; Bucknall, R. Practical Moving Target Detection in Maritime Environments Using Fuzzy Multi-Sensor Data Fusion. *Int. J. Fuzzy Syst.* **2021**, *23*, 1860–1878. [CrossRef]
23. Shi, Z.; Zhen, R.; Liu, J. Fuzzy Logic-Based Modeling Method for Regional Multi-Ship Collision Risk Assessment Considering Impacts of Ship Crossing Angle and Navigational Environment. *Ocean. Eng.* **2022**, *259*, 111847. [CrossRef]
24. Liu, Z.; Xu, J.; Li, J.; Plaza, A.; Zhang, S.; Wang, L. Moving Ship Optimal Association for Maritime Surveillance: Fusing AIS and Sentinel-2 Data. *IEEE Trans. Geosci. Remote Sens.* **2022**, *60*, 5635218. [CrossRef]
25. Cheng, Z.; Zhang, Y.; Wu, B.; Guedes Soares, C. Traffic-Conflict and Fuzzy-Logic-Based Collision Risk Assessment for Constrained Crossing Scenarios of a Ship. *Ocean. Eng.* **2023**, *274*, 114004. [CrossRef]

26. Ojha, V.; Abraham, A.; Snášel, V. Heuristic Design of Fuzzy Inference Systems: A Review of Three Decades of Research. *Eng. Appl. Artif. Intell.* **2019**, *85*, 845–864. [CrossRef]
27. Haghrah, A.A.; Ghaemi, S. PyIT2FLS: A New Python Toolkit for Interval Type 2 Fuzzy Logic Systems. *arXiv* **2019**, arXiv:1909.10051.
28. Huang, J.; Ri, M.; Wu, D.; Ri, S. Interval Type-2 Fuzzy Logic Modeling and Control of a Mobile Two-Wheeled Inverted Pendulum. *IEEE Trans. Fuzzy Syst.* **2018**, *26*, 2030–2038. [CrossRef]
29. Xian, W.; Qi, Q.; Liu, W.; Liu, Y.; Li, D.; Wang, Y. Control of Quadrotor Robot via Optimized Nonlinear Type-2 Fuzzy Fractional PID with Fractional Filter: Theory and Experiment. *Aerosp. Sci. Technol.* **2024**, *151*, 109286. [CrossRef]
30. Acosta, H.; Wu, D.; Forrest, B.M. Fuzzy Experts on Recreational Vessels, a Risk Modelling Approach for Marine Invasions. *Ecol. Model.* **2010**, *221*, 850–863. [CrossRef]
31. Munkres, J. Algorithms for the Assignment and Transportation Problems. *J. Soc. Ind. Appl. Math.* **1957**, *5*, 32–38. [CrossRef]
32. Liu, Z.; Yuan, L.; Weng, L.; Yang, Y. A High Resolution Optical Satellite Image Dataset for Ship Recognition and Some New Baselines. In Proceedings of the 6th International Conference on Pattern Recognition Applications and Methods, Porto, Portugal, 24–26 February 2017; SCITEPRESS—Science and Technology Publications. pp. 324–331.